



## Research article

# Functional and genomic characterization of a wound- and methyl jasmonate-inducible chalcone isomerase in *Eremochloa ophiuroides* [Munro] Hack

Moon-Soo Chung<sup>a</sup>, Gun Woong Lee<sup>a,1</sup>, Yeon Sim Jeong<sup>a</sup>, Yong In Kuk<sup>c</sup>, Seung Sik Lee<sup>a,b</sup>,  
Byung Yeoup Chung<sup>a</sup>, Sungbeom Lee<sup>a,b,\*</sup>

<sup>a</sup> Research Division for Biotechnology, Advanced Radiation Technology Institute, Korea Atomic Energy Research Institute, Jeongseup-si, Jeollabuk-do, 56212, Republic of Korea

<sup>b</sup> Department of Radiation Science and Technology, University of Science and Technology, Daejeon, 34113, Republic of Korea

<sup>c</sup> Department of Oriental Medicine Resources, Suncheon National University, Suncheon-si, Jeollanam-do, 57922, Republic of Korea

## ARTICLE INFO

## Keywords:

Centipede grass  
Chalcone isomerase  
Exon–  
Intron structure  
*Arabidopsis tt5*  
Intron phase

## ABSTRACT

*Eremochloa ophiuroides*, a perennial warm-season lawn grass, has a characteristic phenotype of red pigmentation in tissues during maturation. The putative gene families associated with the red coloration were previously identified in *E. ophiuroides*. These genes encode chalcone synthases, flavonol 3-hydroxylases, and flavonol 3'-hydroxylases, acting on the early flavonoid-biosynthesis pathway. Here, a type-I chalcone isomerase (*CHI*) gene was isolated from *E. ophiuroides* based on leaf-transcriptome data, and the corresponding enzyme was functionally characterized in vitro and in planta. Complementation of *Arabidopsis tt5* mutants by overexpressing *EoCHI* recapitulated the wild-type seed coat color. Wounding and methyl jasmonate treatments significantly elevated the transcript level of *EoCHI* and total anthocyanin content in shoots. Confocal microscopy indicated the localization of *EoCHI* to the endoplasmic reticulum. The genomic *EoCHI* sequence contained two introns with a novel pattern of exon–intron organization. Further examinations on genomic structures of *CHI* family from ancient to advanced plant lineages should be of interests to decipher evolutionary pathways of extant plant *CHI* genes.

## 1. Introduction

Flavonoids are ubiquitous aromatic molecules that constitute one of the major forms of secondary metabolites in plants. Beyond providing pigmentation in flowers, leaves, seeds, and fruits, flavonoids serve broad physiological and biological functions in plant–environment interactions, such as in signaling to attract pollinators and for symbiosis with rhizobacteria, protection against ultraviolet B (UV-B) radiation and pathogen attacks, cell cycle regulation, anti-oxidation, auxin transportation, and for pharmaceutical purposes (promoting health benefits and combatting diseases) (Agati et al., 2013; Falcone Ferreyra et al., 2012; Smith and Luo, 2004; Tapas et al., 2008; Winkel-Shirley, 2001). A series of enzymatic steps lead to flavonoid end-products biosynthesis, starting from enzymes in the early steps such as chalcone synthase (CHS), chalcone isomerase (CHI), flavonol 3-hydroxylase

(F3H), and flavonol 3'-hydroxylase (F3'H) (Winkel-Shirley, 2001).

CHI (EC 5.5.1.6) is one of the key enzymes that provide pigmentation in seed coats, in particular, by catalyzing the stereospecific isomerization of naringenin chalcone (2',4,4',6'-tetrahydroxychalcone; abbreviated as 6'-hydroxychalcone) to naringenin (5,7,4'-trihydroxyflavanone; abbreviated as 5-hydroxyflavanone). Mutation of the *CHI* locus in *Arabidopsis thaliana* (named *transparent testa 5*, or *tt5*) disrupted the synthesis of brown pigments in seed coats (Shirley et al., 1995). However, ectopic overexpression of *CHI* homologs in the *tt5* mutant recapitulated the brown pigmentation of wild-type (WT) *Arabidopsis* seeds (Dong et al., 2001; Kim et al., 2007; Shih et al., 2008). In addition, the absence of *CHI* in rice with a mutation in the golden hull and internode 1 (*gh1*) gene led to extraordinary golden pigmentation in the seed hulls and internodes after light exposure (Hong et al., 2012). These results suggested that a *CHI* played a significant role in coordinating

\* Corresponding author., Research Division for Biotechnology, Advanced Radiation Technology Institute, Korea Atomic Energy Research Institute, Jeongseup-si, Jeollabuk-do, 56212, Republic of Korea.

E-mail address: [sungbeom@kaeri.re.kr](mailto:sungbeom@kaeri.re.kr) (S. Lee).

<sup>1</sup> Present address: Jeonju AgroBio-Materials Institute, Jeonju-si, Jeollabuk-do 54810, Republic of Korea.

<https://doi.org/10.1016/j.plaphy.2019.10.008>

Received 18 May 2019; Received in revised form 6 October 2019; Accepted 6 October 2019

Available online 10 October 2019

0981-9428/ © 2019 Elsevier Masson SAS. All rights reserved.

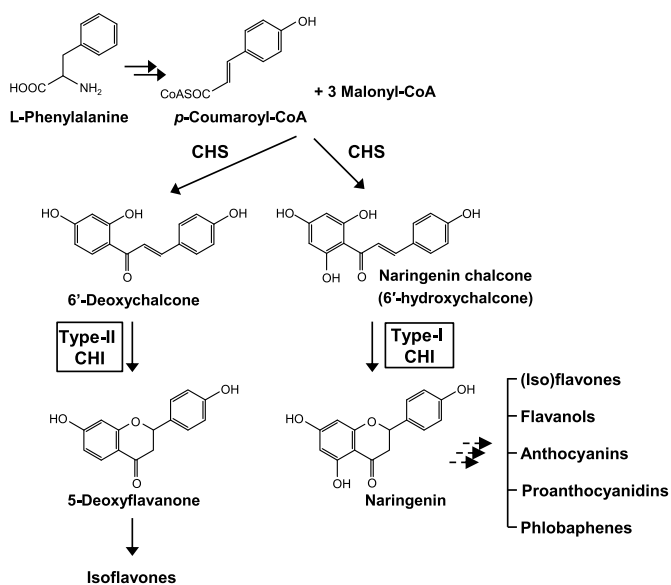


Fig. 1. A simplified route for phenylpropanoid biosynthesis. CHS, a chalcone synthase; CHI, a chalcone isomerase.

metabolic flux from naringenin chalcone to downstream flavonoid biosynthetic pathways.

Depending on substrate preferences, *CHIs* are classified into two types (Dixon et al., 1988). Type-I *CHIs* are found in non-leguminous plants and only isomerize 6'-hydroxychalcone to 5-hydroxyflavanone, whereas type-II *CHIs* are specialized in legume plants and accept both 6'-hydroxychalcone and 6'-deoxychalcone as substrates to produce 5-hydroxyflavanone and 5-deoxyflavanone, respectively (Fig. 1). The *CHI* activities of crude proteins and the functional characterizations of *CHI* complementary DNAs (cDNAs) have been documented in various plant species, including *A. thaliana* (Shirley et al., 1995), *Glycine max* (Bednar and Haddock, 1988), *Zea mays* (Grotewold and Peterson, 1994), *Ipomoea batatas* (Guo et al., 2015), *Saussurea medusa* (Li et al., 2006), *Oryza sativa* (Shih et al., 2008), *Trigonella foenum-graecum* (Qin et al., 2011), *Ginkgo biloba* (Cheng et al., 2011), *Citrus sinensis* (Fouché and Dubery, 1994), *Petunia hybrida* (Van Tunen and Mol, 1987), and *Pueraria lobata* (Terai et al., 1996). Type-II *CHIs* are most likely present only in leguminous plants, some of which have shown the exceptional genomic feature of having both type-I and type-II *CHIs* (Kimura et al., 2001), or a gene cluster with four type-I and -II *CHIs* in *Lotus japonicus* (Shimada et al., 2003). Besides the type-I and type-II *CHIs*, *CHI*-like genes (*CHILs*), known as a type-III and a type-IV *CHIs*, are found in *Arabidopsis* and soybean. A *CHIL* plays a role in enhancing flavonoid production and is known as a fatty acid binding protein, but has no chalcone cyclization activity (Jiang et al., 2015; Morita et al., 2014; Ngaki et al., 2012).

Centipede grass (*Eremochloa ophiuroides* [Munro] Hack.) is a warm-season lawn grass that is widely planted because of its low nitrogen requirements and broad spectrum of climatic conditions to grow. Most (if not all) *E. ophiuroides* (*Eo*) cultivars have characteristic pigmentation in their stolons, spikes, and leaves during maturation (Li et al., 2018a,b). Abiotic stresses such as UV-B, wounds, and ionizing radiation can also induce red pigmentation (mainly with flavonoids accumulation) in the leaves, which significantly suppressed the survival of the fall armyworm (Lee et al., 2012). Methyl jasmonate (MeJA) is known to modulate numerous vital physiological processes, including defense responses against herbivores and pathogens, wound responses, secondary metabolite (e.g., flavonoids) biosynthesis, and flower development and fertility (Cheong and Choi, 2003; Danae et al., 2015; Ghazemzadeh et al., 2016; Wang et al., 2015). Recently, most structural genes in the flavonoid biosynthetic pathway in *Eo* were identified and

annotated by de novo assembly together with comparative-transcriptome analysis between two *Eo* accessions with different pigmentation patterns during development – E092 (red pigmentation accession) and E092-1 (green accession) (Li et al., 2018a,b). Given the higher accumulation of total anthocyanidin in the stolons and spikes of E092 and quantitative confirmation of transcript abundances of candidate genes required for flavonoid biosynthesis, two *CHSs*, four dihydroflavonol-4-reductases (*DFRs*), eight *F3Hs*, and several transcription factors (such as MYB, bHLH, and WD40) were annotated except for a *CHI* that is another key gene positioned in the early pathway of flavonoid biosynthesis.

In this study, we aimed to identify a missing key gene, i.e., a *CHI*, in a flavonoid biosynthetic pathway in *Eo*. Using our de novo transcriptome data collected from the shoots of *Eo*, *CHIs* were identified and functionally characterized in vitro and in planta. We examined induced *CHI* expression and accumulation of total anthocyanin contents upon the elicitations by MeJA treatment and mechanical wounding. Our findings provide substantial information regarding a biochemical step important for the coloration of seed coats and red pigmentation in *Eo* tissues. Moreover, a novel genomic structure was found in the *CHI* gene, which will open the door for elucidating the evolutionary pathways of plant *CHI* genes.

## 2. Materials and methods

### 2.1. Plant materials and abiotic stress treatments

*Arabidopsis* plants (Columbia-0) were grown in an in-house growth room maintained at 22 °C, with 60–70% relative humidity, a day/night photoperiod of 16 h/8 h, and a light density of 100–150  $\mu\text{mol m}^{-2} \text{s}^{-1}$ . Seeds were imbibed at 22 °C for 30 min, followed by surface-sterilization for 5 min with 70% (v/v) ethanol and for 10 min with 2% (v/v) sodium hypochlorite. After five washes with sterile deionized water, the seeds were germinated on 0.6% (w/v) phytoagar solid medium containing half-strength Murashige and Skoog salts (MS) salts with vitamins and 1.5% (w/v) sucrose. Then, the germinated seeds were incubated at 4 °C in the dark for 3 days to allow for stratification. Transformed seeds were selected in a half-strength MS plate, supplemented with 15  $\text{mg L}^{-1}$  phosphinothricin and 50  $\text{mg L}^{-1}$  cefotaxime. An *Arabidopsis chi* knock-out mutant (*tt5*, CS300857) was obtained from the *Arabidopsis* Biological Resource Center (The Ohio State University, OH, USA). Centipede grass seeds were purchased from Fukukaen Nursery (Blu Co. Ltd., Nagoya, Japan) and cultivated in a plant growth chamber (28 °C, 60% of relative humidity, 16 h/8 h of day/night photoperiod, and light intensity of 100–110  $\mu\text{mol m}^{-2} \text{s}^{-1}$ ).

MeJA (50  $\mu\text{M}$ ) and dimethylsulfoxide (50  $\mu\text{M}$ , control) were used to treat 3-month-old *Eo* plants using the foliar-spray method, supplementing with 0.05% (v/v) Tween-20. The leaves were harvested at 3, 5, 7, and 10 days after the treatments and stored at  $-80\text{ }^{\circ}\text{C}$  until use. Wound was treated with cross-sectional folding in the middle of intact leaves of 3-month-old *Eo* plants. The part above each wounding site (W2) showed red pigmentation, whereas the part below (W1) showed no pigmentation. Each part was harvested at 7 days after wound treatment and stored at  $-80\text{ }^{\circ}\text{C}$  until use.

### 2.2. mRNA sequencing and de novo transcriptome assembly

Total RNA was extracted from the aerial parts (without stolons and spikes) of 3-month-old *Eo* plants using the RNeasy® Plant Mini Kit (Qiagen, CA, USA) with RNase-Free DNase Set (Qiagen) according to the manufacturer's instructions, and mRNA samples were purified using poly-T oligo-conjugated magnetic beads. mRNA sequencing was performed using the Illumina platform (HISEQ 2500 sequencing system). Paired-end sequence files obtained from the shoots of *Eo* were processed using Trimmomatic-0.32 software. Total preprocessed sequences were pooled and assembled using the Trinity assembler (Grabherr et al.,

**Table 1**  
Primers used in this study.

	Sequence (5' to 3')	
	Forward	Reverse
For genomic PCR		
<i>EoCHI</i> _Full	ATGGCCGTTTCGGAGGTGGTC	TCAGGCGTTGACCGAGACGGG
For genotyping PCR for <i>tt5</i>		
<i>chi</i> (P1 + P2)	GTGCGTTTGAGAAGTTTATC	CTTTATTATAATGTAAATGC
<i>chi</i> (P1 + P3)	GTGCGTTTGAGAAGTTTATC	ATATTGACCATCATACTCATTGC
For RT-PCR and qPCR		
<i>AtCHI</i>	GTGCGTTTGAGAAGTTTATC	CTTTATTATAATGTAAATGC
<i>AtACT2</i>	ATTCAGATGCCAGAAGTCTTGT	GAAACATTTCTGTGAACGATTCT
<i>EoCHI</i>	GTCCGAGCTCCTGACCAAGG	GGCATCCACGCATGCAAGG
<i>EoACT</i>	CGTACCACAGGTATCGTGC	CCTTGCTCATCTGTGACG
<i>EoTUB</i>	GTCCTGTCCACCCACTCC	CTGCGGTTGCACCTTGG

2011), with the default settings. The CD-HIT-EST program was used to remove redundant sequences with 95% sequence similarity (Huang et al., 2010). Finally, the assembled transcripts ( $\geq 500$  base pairs [bp]) were used as the reference transcriptome and were functionally annotated using BLASTX mapping (e-value cut-off of  $1e^{-5}$ ) against the UniProt KB database (Viridiplantae) and the Kyoto Encyclopedia of Genes and Genomes (KEGG) pathway maps. In addition, the Gene Ontology (GO) terms were assigned using Blast2GO (Conesa et al., 2005).

### 2.3. Accession numbers

We deposited the RNA-Seq data obtained in this study in the NCBI Sequence Read Archive (SRA) under SRA accession number PRJNA515087 (SAMN10724124–SAMN10724131).

### 2.4. Amplification of the *EoCHI* genomic fragment

Genomic DNAs of *Eo* were isolated from leaf tissues using the Exgene™ Plant SV Mini Kit (GeneAll, Seoul, Republic of Korea), following the manufacturer's instructions. To amplify a genomic fragment of *EoCHI*, a pair of primers (*EoCHI*\_Full, see Table 1 for sequence information) was designed based on the mRNA sequences of ISGT\_1238 that were predicted as a *CHI* gene, using de novo RNA sequence assembly and annotations. A polymerase chain reaction (PCR) was performed using Phusion® High-Fidelity DNA Polymerase (New England BioLabs, MA, USA), with 35 cycles of 94 °C, 30 s; 55 °C, 30 s; and 72 °C, 1 min. The amplicon was purified using Expin™ Gel SV Kit (GeneAll) and cloned into the pJET1.2/blunt vector (Thermo Fisher, MA, USA). The amplicon sequence was confirmed in both directions.

### 2.5. Expression of the recombinant *EoCHI* protein and in vitro enzyme assays

The first-strand cDNAs were synthesized using 1 µg of total RNA of leaf tissues with a LaboPass™ cDNA Synthesis Kit (Cosmogenetech, Seoul, Republic of Korea). The complete coding region of *EoCHI* was amplified by using Phusion® High-Fidelity DNA Polymerase with the primers, 5'-ggatccatggccgtttcggaggtggtc-3' (forward-*Bam*HI) and 5'-aagcttcaggcgttgaccgagac-3' (reverse-*Hind*III), and the resulting amplicon was cloned into the pJET1.2/blunt vector, generating the *EoCHI*/pJET1.2 construct (for sequencing), or into a pET-28a(+) vector (Novagen, WI, USA) for overexpression of the recombinant protein. After confirming the *EoCHI* sequences in both strands, the constructs were introduced in *Escherichia coli* BL21 (DE3) and overexpressed via induction in the presence of 0.5 mM isopropyl  $\beta$ -D-1-thiogalactopyranoside at 16 °C for 20 h. The cells were then harvested by centrifugation at  $5000 \times g$  for 15 min at 4 °C, and the cell pellet was

suspended in phosphate-buffered saline containing 1 mM phenylmethanesulfonyl fluoride. After cell disruption by sonication, a soluble fraction was purified using TALON metal affinity chromatography resin (Clontech, CA, USA). Protein concentration was estimated by the Bradford assay, using bovine serum albumin as a calibration standard.

Enzymatic activity of CHI was determined as previously described method with minor modifications (Cheng et al., 2011). In vitro assays were performed at 30 °C for 10 min in a 500 µL reaction volume containing 50 mM Tris-HCl buffer (pH 5.2), 150 µM naringenin chalcone or 150 µM 6'-deoxychalcone, and 10 µg purified protein. As a negative control reaction, heat (90 °C)-denatured recombinant proteins were used instead, with identical reaction conditions. The reaction products were extracted twice with an equal volume of ethyl acetate, followed by centrifugation at  $10,000 \times g$  for 20 min. After vacuum-drying, each pellet was dissolved in 100 µL of ethanol, and a 10 µL aliquot was analyzed on an Agilent 1200 Series HPLC System (Agilent Technologies, Tokyo, Japan), equipped with an YMC-Pack ODS-A column ( $4.6 \times 150$  mm, particle size 5 µm, YMC America, PA, USA). The mobile phase consisted of 40% (v/v) methanol (A) and 3% (v/v) acetic acid in water (B), the flow rate was  $1 \text{ mL min}^{-1}$ , and the temperature was 40 °C. Each eluate was monitored at 304 nm during isocratic elution with 30% B for 1 h, and the retention time of each peak was compared with those of authentic standards. Naringenin, 6'-deoxychalcone, and 5-deoxyflavanone were purchased from Sigma–Aldrich (MO, USA). Naringenin chalcone was purchased from ChemFaces (Hubei, PRC).

### 2.6. Complementation of the *Arabidopsis tt5* mutant

To confirm the functionality of *EoCHI* in planta, full-length of *EoCHI* cDNA was introduced into the *tt5* mutant of *Arabidopsis*. The complete coding region of *EoCHI* was amplified using the *EoCHI*/pJET1.2 plasmid as a template with the primer set, 5'-caccatggccgtttcggaggtggtc-3' (forward) and 5'-tcaggcgttgaccgagacggg-3' (reverse). A plant expression vector (pB7WG2) was generated via the pENTR™/D-TOPO® vector (Invitrogen, CA, USA) using Gateway™ LR Clonase™ II Enzyme Mix (Invitrogen) (Karimi et al., 2002). After sequence confirmation by automated DNA sequencing in both directions, the resulting construct was then introduced into a homozygous *tt5* mutant by an *Agrobacterium*-mediated floral dipping method (Clough and Bent, 1998). The colors of the seed coats were visualized with a Leica EZ4E stereo microscope (Leica microsystems, Heerbrugg, Switzerland).

### 2.7. Reverse transcription (RT)-PCR and quantitative real-time PCR (qRT-PCR)

One microgram of total RNAs extracted from control *Eo*, the wound- and MeJA-treated *Eo*, and transgenic *Arabidopsis* plants was reverse

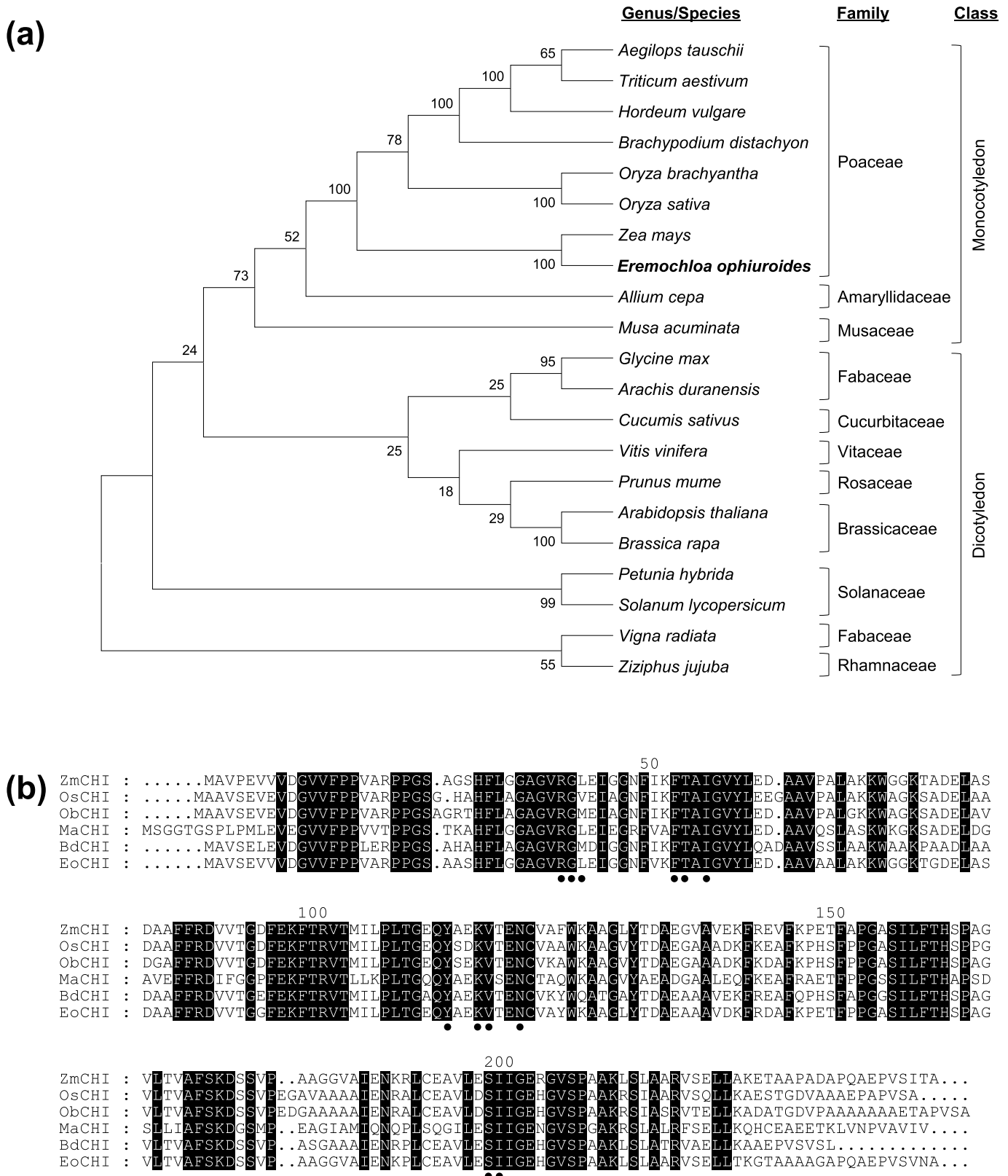


**Fig. 2.** Phylogenetic analysis and comparison of the deduced amino acid sequences of plant CHIs. (a) Phylogenetic analysis of *EoCHI* and known plant CHIs. *A. tauschii*, AHI94948.1; *A. cepa*, AAU11843.1; *A. thaliana*, NP\_191,072.1; *A. duranensis*, XP\_015942314.1; *B. distachyon*, XP\_003559241.1; *B. rapa*, XP\_009116213.1; *C. sativus*, XP\_004149817.1; *G. max*, NP\_001236768.1; *H. vulgare*, AAM13449.1; *M. acuminata*, XP\_009396862.1; *O. brachyantha*, XP\_006650802.1; *O. sativa*, XP\_015628287.1; *P. hybrida*, CAA32730.1; *P. mume*, XP\_008233532.1; *S. lycopersicum*, NP\_001307640.1; *T. aestivum*, AFJ38178.1; *V. radiata*, NP\_001304223.1; *V. vinifera*, NP\_001268033.1; *Z. mays*, NP\_001144002.2; and *Z. jujube*, XP\_015877061.1. The unrooted tree was aligned and visualized using MEGA 6 software with the neighbor-joining algorithms (1000 bootstrap replications). (b) Alignment of the deduced amino acid sequence of *EoCHI* with those of known CHIs from monocot plants. The black dots indicate the residues that are conserved in CHI active sites (Jez et al., 2000).

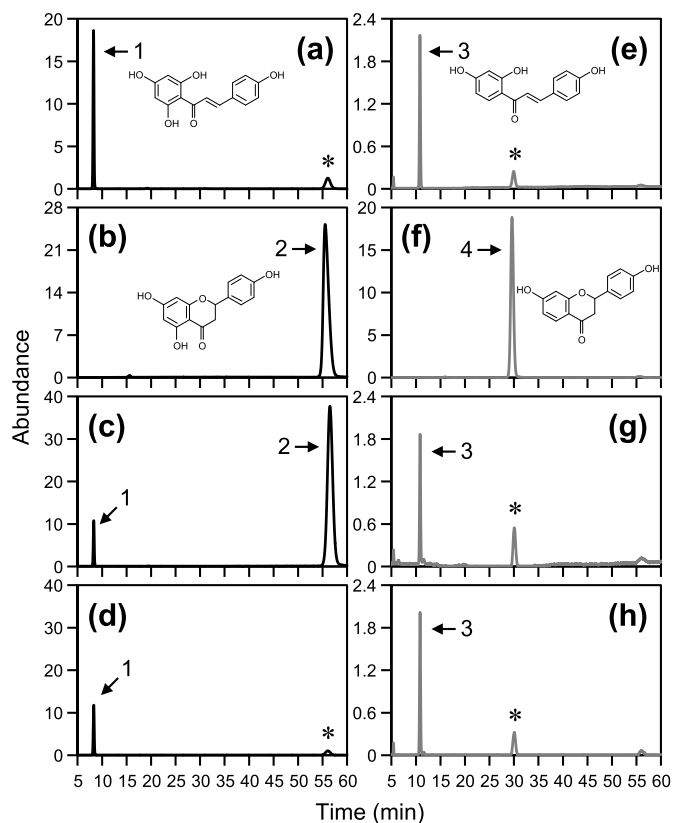


**Fig. 3.** HPLC chromatograms of reaction products from in vitro enzyme assays. (a–b) and (e–f), Authentic standards of (1) naringenin chalcone (2  $\mu$ g), (2) naringenin (4 ng), (3) 6'-deoxychalcone (2  $\mu$ g), and (4) 5-dexoyflavanone (4 ng), respectively. (c) and (g), In vitro enzyme assays with recombinant *EoCHI* using naringenin chalcone and 6'-deoxychalcone as substrates, respectively. (d) and (h), In vitro assays using heat-denatured *EoCHI* as negative controls. '\*' represents a peak from the impurity of naringenin and 6'-deoxychalcone authentic standard solutions.

transcribed using a LaboPass™ cDNA Synthesis Kit. PCR was conducted as follows: 95 °C (5 min); 25–28 cycles of 95 °C (30 s)/58 °C (30 s)/72 °C (30 s); and a final extension at 72 °C (5 min). The PCR products were visualized on a 1.5% (w/v) agarose gel, which was stained with GelRed™ Nucleic Acid Gel Stain (Biotium, CA, USA). The number of PCR cycles for each primer pair was optimized by determining the number of cycles, at which the amplifications occur exponentially (28 cycles for *EoCHI* and *AtCHI*, and 25 cycles for *Arabidopsis* actin 2 [*AtACT2*]). *AtACT2* was detected as an endogenous control gene. Quantitative RT–PCR was conducted as follows: 95 °C (30 s) and 40 cycles of 95 °C (15 s)/60 °C (60 s). Two endogenous control genes (*Eo* actin [*EoACT*] and *Eo* tubulin [*EoTUB*]) were used, and quantitative analyses were performed via comparative quantification of the amplified products using the  $2^{-\Delta\Delta C_T}$  method, with an Applied Biosystems 7300 Real-Time PCR System (Applied Biosystems, CA, USA) and the SYBR Green intercalating dye for fluorescence detection (Bio-Rad, CA, USA). The oligonucleotide sequences of the primers used for RT–PCR and qRT–PCR are presented in Table 1. RT–PCR and qRT–PCR analyses were conducted in triplicate using independent biological samples.

## 2.8. Quantification of total anthocyanin content

Extraction and determination of anthocyanins were performed according to the previously described methods (Mohamed et al., 2016; Shin et al., 2007). For anthocyanin extraction, 100 mg of samples were pulverized and mixed in 1 ml of extraction buffer [methanol containing 1% (v/v) HCl] and were incubated for 18 h at 4 °C in the dark. The

anthocyanin extract was centrifuged separately at 10,000  $\times$  g for 10 min at 4 °C and was diluted with buffer solutions at pH 1.0 (25 mM KCl) and at pH 4.5 (0.4 M sodium acetate). Absorbance of each sample was measured at 520 and 700 nm with Evolution™ 300 UV-VIS Spectrophotometer (Thermo Fisher, WI, USA) and the anthocyanin content was estimated by a pH differential method. The total anthocyanin content (g/L) was expressed as cyanidin-3-glucoside according to the following equation and was converted to micrograms of anthocyanin per gram fresh weight:

$$\text{Anthocyanin pigment (g/L)} = (A \times \text{MW} \times \text{DF}) / (\epsilon \times l)$$

where:

$$A = (A_{520\text{nm}} - A_{700\text{nm}})_{\text{pH}1.0} - (A_{520\text{nm}} - A_{700\text{nm}})_{\text{pH}4.5}$$

MW = 449.2 g/mol for cyanidin-3-glucoside

DF = dilution factor,  $\epsilon$  = molar absorptivity of cyanidin-3-glucoside (26,900),  $l$  = cell path length (1 cm).

## 2.9. Confocal microscopy

The full-length *EoCHI* cDNA fragment was amplified using the *EoCHI*/pJET1.2 construct as a template with the primers, 5'-cacatggcgttttcgaggtggc-3' (forward) and 5'-ggcgttgaccgagacggg-3' (reverse). The amplicon was cloned into the pB7FWG2 vector via the pENTR™/D-TOPO® vector with the Gateway™ LR Clonase™ II Enzyme Mix. After sequence confirmation, the construct was transiently expressed in tobacco leaves (*Nicotiana benthamiana*) (Yang et al., 2000). Recombinant *Brassica rapa* delta-12 fatty acid desaturase 2-1 (BrFAD2-1) fused with monomeric red fluorescent protein (mRFP) was used as an endoplasmic reticulum (ER) marker protein (Jung et al., 2011). An empty pGWB554 vector was used for cytosolic expression marker (Nakagawa et al., 2007), which expresses a non-coding 100-bp fragment fused with mRFP for inactivation of a *ccdB* gene. Tobacco leaves co-expressing an *EoCHI*:enhanced green fluorescent protein (EGFP) fusion protein and BrFAD2-1:mRFP were visualized using an LSM 800 laser-scanning confocal microscope (Carl Zeiss AG, Oberkochen, Germany) with a Plan-Apochromat 20  $\times$  /0.8 M27 objective and sequential scanning at excitation/emission  $\lambda_s$  (nm) = 488/509 (for EGFP) and 561/612 (for mRFP). The fluorescence images were obtained and processed using ZEN 2012 SP2 software (Carl Zeiss).

## 2.10. Sequence alignment, phylogenetic tree construction, and intron phase analysis

The deduced amino acid sequence of *EoCHI* was aligned with those of known plant CHIs obtained from the National Center for Biotechnology Information (NCBI): *Aegilops tauschii*, AHI94948.1; *Allium cepa*, AAU11843.1; *A. thaliana*, NP\_191,072.1; *Arachis duranensis*, XP\_015942314.1; *Brachypodium distachyon*, XP\_003559241.1; *B. rapa*, XP\_009116213.1; *Cucumis sativus*, XP\_004149817.1; *G. max*, NP\_001236768.1; *Hordeum vulgare*, AAM13449.1; *Musa acuminata*, XP\_009396862.1; *Oryza brachyantha*, XP\_006650802.1; *O. sativa*, XP\_015628287.1; *P. hybrida*, CAA32730.1; *Prunus mume*, XP\_008233532.1; *Solanum lycopersicum*, NP\_001307640.1; *Triticum aestivum*, AFJ38178.1; *Vigna radiata*, NP\_001304223.1; *Vitis vinifera*, NP\_001268033.1; *Z. mays*, NP\_001144002.2; and *Ziziphus jujube*, XP\_015877061.1. Amino acid sequences were aligned using the DNA Star package (Laser gene, WI, USA) and visualized using GeneDoc (<http://www.psc.edu/biomed/genedoc>). A phylogenetic tree was constructed using Molecular Evolution Genetics Analysis (MEGA) software version 6 with the neighbor-joining algorithm (1000 bootstrap replications and handling gaps with pairwise deletion). Intron phases were defined as described previously (Trapp and Croteau, 2001).

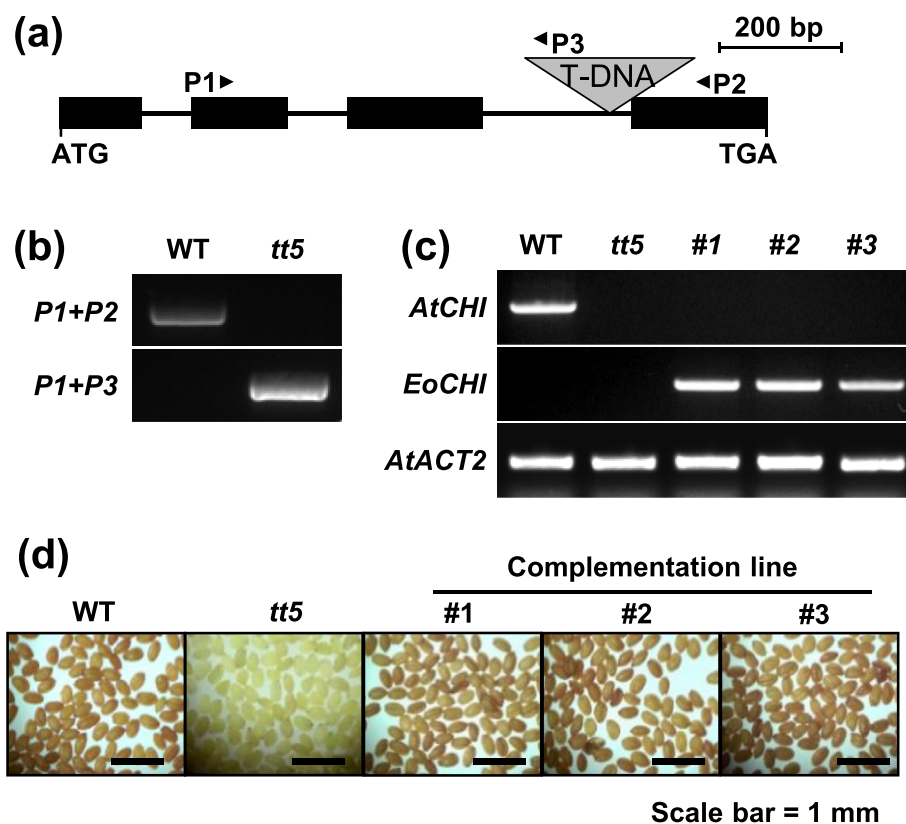


Fig. 4. In planta functional characterization of *EoCHI*. (a) Schematic representation of the genomic structure of a null *Arabidopsis tt5* mutant. The relative locations of a T-DNA insertions and the primers used in genotyping assays are indicated. (b) Genomic PCR for genotype confirmation for the *tt5* mutants. (c) Determination of *EoCHI* transcript levels in WT (Col-0); *tt5*; and #1, #2, and #3 (three biologically independent *tt5* mutants overexpressing *EoCHI* cDNA). *AtACT2* was used as an endogenous control gene. (d) Images of the seeds harvested from the WT, *tt5*, and complementation lines shown in Fig. 4c.

### 3. Results

#### 3.1. A de novo transcriptome assembly identified a type-I CHI gene

To identify a *CHI* gene, we constructed a de novo transcript assembly using the aerial tissues (mainly leaves without stolons and spikes) of *Eo*. The de novo transcriptome was comprised of 46,552 contigs (minimum, 500 bp; maximum, 16,298 bp; average, 1091 bp) after removing redundant sequences and low-quality sequences from 53,066 initial contigs. Seven contigs were annotated as *CHI* mRNA sequences: ISGT\_1238 (986 bp), ISGT\_9433 (996 bp), ISGT\_44,473 (580 bp), ISGT\_11,943 (1219 bp), ISGT\_37,547 (853 bp), ISGT\_2962 (1674 bp), and ISGT\_4075 (1174 bp). Among these, both ISGT\_1238 and ISGT\_11,943 contained the entire protein-coding sequences, translating into 231 amino acids (23.61 kDa, isoelectric point of 4.896) and 223 amino acids (23.59 kDa, isoelectric point of 4.544), respectively, which were comparable to those of known CHIs (Druka et al., 2003; Li et al., 2006; Soderlund et al., 2009). The other contigs were either redundant or partial sequences. A maize CHI protein was the most closely related to ISGT\_1238 in BLAST analysis with amino acid sequence identity (90.9%), followed by *B. distachyon* (79.3%), *O. sativa* (76.8%), and *O. brachyantha* (74.8%) (Fig. 2a and Supplementary Fig. A1). In contrast, ISGT\_11,943 was closely related to known CHILs found in *Z. mays* (84.4%), *O. sativa* (72.3%), *G. max* (57.3%), and *A. thaliana* (57.2%). The ISGT\_11,943 protein has no conserved catalytic residues found in typical CHIs (Supplementary Fig. A2). The initial PCR primers were designed based on the ISGT\_1238 mRNA sequences to amplify genomic and cDNA fragments of *EoCHI* (Table 1). Genomic PCR and RT-PCR assays generated single amplicons of 976 bp (genomic fragment) and 696 bp (cDNA), respectively. The deduced sequence of *EoCHI* revealed amino acids that are conserved at active sites in type-I CHIs in higher plants (Jez et al., 2000). Those amino acids in *EoCHI* included Arg-34, Gly-35, Leu-36, Phe-45, Thr-46, and Ile-48 within the large, N-terminal  $\beta$ -sheets and Tyr-104, Lys-107, Val-108, Asn-111, Ser-188, and Ile-189 within  $\alpha$ -helices (Fig. 2b). Based on the active site residues of Ser-188

and Ile-189, which are known as determinants for the substrate preference for 6'-hydroxychalcone, *EoCHI* was classified as a type-I CHI: replacement with Thr-188 and Met-189 would result in a predicted substrate preference for 6'-deoxychalcone found in type-II CHIs (Jez et al., 2000).

#### 3.2. Functional characterization of ISGT\_1238 as a CHI

To determine the functional activities conferred by ISGT\_1238, annotated as a putative CHI in our transcriptome analysis, *EoCHI* cDNA was expressed in *E. coli* and purified recombinant proteins were assayed for catalytic activities in isomerizing 6'-hydroxychalcone (naringenin chalcone) and 6'-deoxychalcone into 5-hydroxyflavanone (naringenin) and 5-deoxyflavanone in vitro, respectively. Reaction products generated by the assay were analyzed by high-performance liquid chromatography (HPLC) and identified in comparison with the retention times of authentic standards. Because naringenin chalcone can easily and spontaneously rearrange to form naringenin above pH 5.5, the pH in the assay buffer was set as pH 5.2 (Supplementary Fig. A3) (Mol et al., 1985). While the intact *EoCHI* was able to isomerize naringenin chalcone into naringenin as a single reaction product in vitro, no reaction product was formed using 6'-deoxychalcone as a substrate or heat-denatured *EoCHI* protein (Fig. 3). Therefore, our data clearly demonstrated that the naringenin in the reaction was produced by *EoCHI*-catalyzed enzymatic transformation and that *EoCHI* is a type-I CHI.

#### 3.3. Complementation of *EoCHI* cDNA in the *Arabidopsis tt5* mutant

Eleven loci that modulate flavonoid biosynthesis in *Arabidopsis* have been identified, based on altered pigmentation (yellow or pale brown) in seed coats (Koornneef, 1990). The *CHI* in *Arabidopsis* was correlated with a single-copy *tt5* locus, the absence of which was associated with an altered seed color as well (Shirley et al., 1995). To characterize the functionality of *EoCHI* in planta, the full-length cDNA of *EoCHI* was constitutively expressed under the control of the 35S promoter in

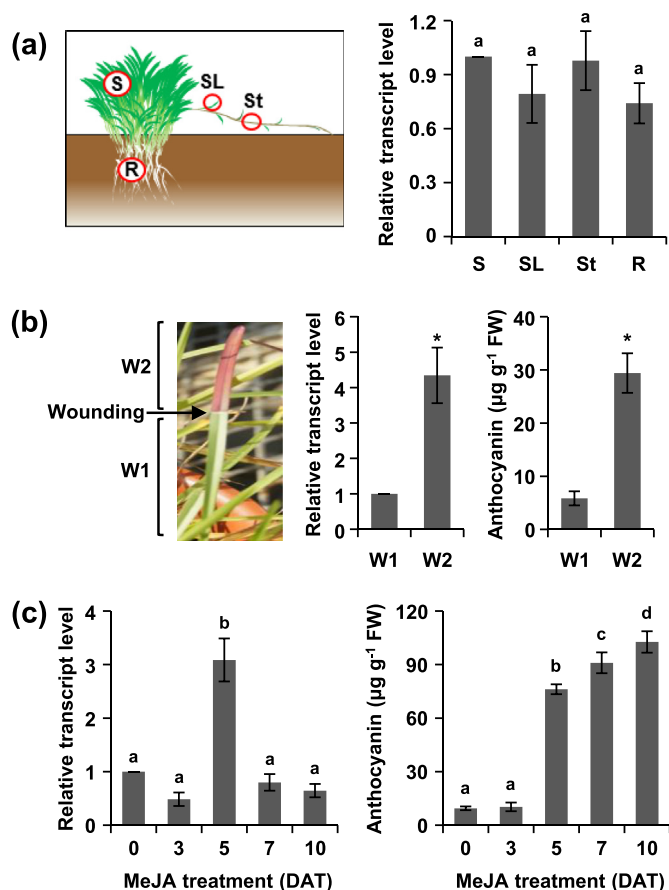


**Fig. 5.** Quantification of transcript levels of *EoCHI* and total anthocyanin contents in various tissues and in response to abiotic stresses. (a) Quantitative transcript levels of *EoCHI* in different tissues. S, shoots; SL, stolon leaves; St, stolons; and R, roots. (b) qRT-PCR analyses of *EoCHI* expression and total anthocyanin contents after wound treatment. An image indicates red pigmentation in centipedegrass shoots after wound treatment, photographed at 7 days after wound treatment. (c) qRT-PCR analyses for *EoCHI* expression and the anthocyanin contents in response to MeJA (50 µM) treatment for the indicated times. Values are means ± SD ( $n = 10$ ) in triplicate. The asterisks (\*) and letters on top of the bar indicate significant differences ( $P < 0.05$ ), as determined by Student's *t*-test and one-way analysis of variance with the Tukey's honestly significant difference test, respectively. Expression levels of two endogenous control genes (*actin* and *tubulin*) were measured to normalize the levels of *EoCHI* mRNAs.

*Arabidopsis tt5* mutants. Interestingly, the testa color of the seeds harvested from the *EoCHI*-overexpressing transgenic *tt5* plants recapitulated the brown color of WT *Arabidopsis* seed coats, as documented in the previous studies (Dong et al., 2001; Hong et al., 2012; Kim et al., 2007). It thus indicated that *EoCHI* was properly expressed and capable of functioning as a CHI in planta (Fig. 4).

### 3.4. Transcript abundances and total anthocyanin content in various tissues and inducible expression by wound and MeJA treatments

The steady-state transcript levels for *EoCHI* were measured by performing qRT-PCR assays with different tissues, including shoots (S), stolon leaves (SL), stolons (St), and roots (R). Transcript levels were normalized relative to those of multiple endogenous control genes such as *ACT2* and *TUB* in each sample. The transcript abundances of *EoCHI* were not significantly different between the tissues of S, SL, St and R (Fig. 5a). However, wound treatment not only increased *EoCHI* transcript level, but also induced red pigmentation in the W2 region, where more than three folds of total anthocyanin contents was accumulated in

comparison to W1 region (Fig. 5b). In addition, exogenous MeJA treatment as a mimic of herbivore attack (Moore et al., 2003) transiently increased the level of *EoCHI* transcripts at 5 days post-treatment. On the contrary, total anthocyanin content was continuously increased at 5 days until 10 days after MeJA treatment (Fig. 5c).

### 3.5. Localization of *EoCHI* in the ER

The presence of CHI enzyme activities was mainly found in cytosolic fractions of protoplasts from *Hippeastrum* petals (Hrazdina et al., 1978). Moreover, immuno-electron microscopy revealed that *Arabidopsis* CHI was associated with cytosolic face of ER (Saslowky and Winkel-Shirley, 2001). To investigate the subcellular localization of *EoCHI*, the full-length *EoCHI* protein fused with EGFP (*EoCHI*:EGFP) was transiently expressed in tobacco leaves by *Agrobacterium*-mediated transformation and compared with the localization of the known ER marker, BrFAD2-1 (Jung et al., 2011), and with that of an empty pGWB554 vector for a cytosolic maker. Confocal microscopy strongly suggested that *EoCHI* was localized to ER, as evidenced by the co-localization of *EoCHI*:EGFP with BrFAD2-1:mRFP (Fig. 6), but not with the localization of cytoplasmic marker.

### 3.6. Genomic organization of the *CHI* gene in *Eo*

A genomic fragment of *EoCHI* (*gEoCHI*) appeared to have three exons and two introns (Table 2), both of which had identical nucleotide lengths (140 bp). To analyze exon-intron organizations, we obtained the genomic sequences of plant *CHIs* from monocots and dicots from the NCBI or the illustrated genomic structures from a previous report (Shoeva et al., 2014). The genomic structure of *EoCHI* appeared relatively well conserved with those of *B. distachyon*, *T. aestivum*, *A. tauschii*, and *H. vulgare* from monocots, as well as *A. duranensis* and *G. max* from dicots in different exons and introns. Intron phasing is defined as phase 0, 1, or 2 based on how codons are split between two exons across intron boundaries (Long et al., 1995). While most (if not all) plant *CHI* genes showed a loss of either intron 1 or intron 3, *gEoCHI* contained a unique loss of intron 2. No similar observation of a loss of intron 2 has been reported for plant *CHI* genes, although an intronless *CHI* gene from *P. hybrida* (X14589) has been documented (Shoeva et al., 2014).

## 4. Discussion

Several key genes positioned in the early pathway of flavonoid biosynthesis were previously annotated in *Eo*, including two *CHSs*, four *DFRs*, and eight of *F3Hs* by analyzing the mixed transcriptomes of leaves, stolons, and spikes (Li et al., 2018a,b). However, a *CHI*, another key gene in the pathway, was not identified previously. In this study, we identified a full-length type-I *CHI* gene and a *CHIL* using *Eo* leaf transcriptome data. We further characterized biochemical functionalities of *EoCHI* in vitro enzyme assays, where purified recombinant proteins of *EoCHI* was able to convert naringenin chalcone into naringenin, thus designating it as an *EoCHI*. To further confirm the functionality of *EoCHI* as a CHI, it was constitutively overexpressed in the *Arabidopsis tt5* mutant, the seeds of which showed an altered color of yellow or pale brown. The brown seeds harvested from the *EoCHI*-overexpressing *tt5* mutants demonstrated that it properly functioned as a CHI by transforming naringenin chalcone to naringenin in planta, as shown in previous studies (Hong et al., 2012; Kim et al., 2007).

In a phylogenetic tree for *CHIs* assembled by the neighbor-joining algorithm, *EoCHI* was most closely related to a maize CHI in the group of type-I *CHIs* (from non-legumes). Based on the characteristic residues for each type of CHI, *EoCHI* was classified as a type-I CHI that were appeared to have a Ser and an Ile (e.g., Ser-188 and Ile-189) in the active site located at the  $\alpha$ -helix ( $\alpha 6$ ) near the C-terminus, elucidated by the crystal structure of alfalfa CHI, rather than corresponding Thr and Met typical of type-II *CHIs* (Jez et al., 2000). *EoCHI* appeared to localize

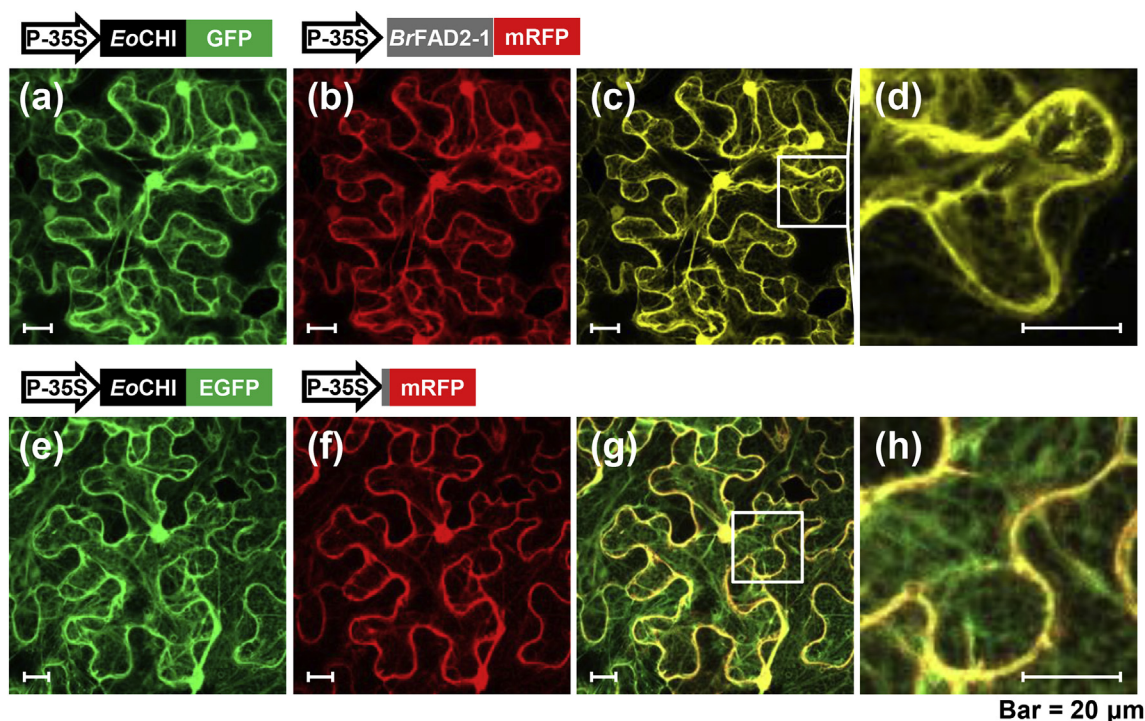


**Fig. 6.** Confocal images of epidermal cells in *N. benthamiana* leaves. (a–d) Confocal images of (a) *EoCHI*:EGFP and (b) a marker for ER localization. (e–h) Confocal images of (e) *EoCHI*:EGFP and (f) a cytosolic marker using pGWB554 vector fused with mRFP. White boxes in (c) and (g) indicated the regions that were shown in (d) and (h), respectively. At least six different cells were examined and only representative images are shown.

**Table 2**

Comparison of intron phases of genomic *EoCHI* with known plant chalcone isomerase genes.

Class	Species <sup>a</sup>	Phase			Genomic structure
		Intron 1	Intron 2	Intron 3	
Monocot	<i>B. distachyon</i>	Loss	2	0	
	<i>M. acuminata</i>	2	2	0	
	<i>O. brachyantha</i>	2	2	0	
	<i>O. sativa</i>	2	2	0	
	<i>Z. mays</i>	2	2	0	
	<i>T. aestivum</i>	2	2	Loss	
	<i>A. tauschii</i>	2	2	Loss	
	<i>H. vulgare</i>	2	2	Loss	
	<i>A. cepa</i>	2	2	0	
	<i>E. ophiuroides</i>	2	Loss	0	
Dicot	<i>A. thaliana</i>	2	2	0	
	<i>A. duranensis</i>	Loss	2	0	
	<i>B. rapa</i>	2	2	0	
	<i>C. sativus</i>	2	2	0	
	<i>G. max</i>	Loss	2	0	
	<i>P. hybrida</i>	2	2	0	
	<i>P. mume</i>	2	2	0	
	<i>S. lycopersicum</i>	2	2	0	
	<i>V. radiata</i>	2	2	0	
	<i>V. vinifera</i>	2	2	0	
	<i>Z. jujuba</i>	2	2	0	

<sup>a</sup> Plant species analyzed in the phylogenetic tree.

to the ER in this study, and the exact localization would most likely be the cytosolic face of the ER, based on a previous localization study of CHI in *Arabidopsis* roots (Saslowky and Winkel-Shirley, 2001).

Inducible accumulation of *CHI* mRNA by biotic and abiotic stresses have been widely documented in many other studies. For example,

fungal elicitor or wound treatment in cell cultures of a legume (*Phaseolus vulgaris*) resulted in the rapid accumulation of steady-state *CHI* transcripts within 3–4 h. In addition, fungal pathogen infection of *Colletotrichum lindemuthianum* in the hypocotyls of the legume induced *CHI* mRNA accumulation after 67–139 h of spore inoculation, depending on compatibilities (Mehdy and Lamb, 1987). In cell suspensions of a medicinal plant (*Hypericum perforatum*), jasmonic acid elicited a 6–8-fold increase of CHI enzyme activity at 4 days post-elicitation (Gadzovska et al., 2007). In this study, we observed more than 3-fold induction of *CHI* mRNA accumulation after wound and MeJA treatments. Consequently, this increment was positively correlated with accumulation of total anthocyanin contents.

The genomic structures of *CHIs* have been comparatively studied among limited lineages of monocots and dicots (Druka et al., 2003; Shoeva et al., 2014). Nonetheless, all of them examined harbored 2 to 3 introns with intron loss observed at either intron 1 or 3, except for one instance where no introns were found in a *P. hybrida* *CHI* gene. Given the intron phasing, however, *EoCHI* appeared to share the conserved patterns observed with other *CHIs*. The number of introns did not directly correlate with cotyledonous types, but most of the *CHI* genes within dicots possessed three introns, except for *A. duranensis* and *G. max* (Table 2). Given the phasing and spatial positioning of each intron, *gEoCHI* appeared to be very well conserved with all the other *CHI* genes examined, containing intron phases of 2 and 0 for introns 1 and 3, respectively (Table 2).

The discovery of intron 2 loss in *EoCHI* indicates that further research should be undertaken to decipher evolutionary pathways in terms of intron–exon structures and the intron phasing of *CHI* genes by including more genomic structures of *CHI* genes from various taxa, including ancestral, intermediate, and advanced plant species in the molecular phylogeny tree.

#### Author contribution

S.L. and M.-S.C. conceived and designed all experiments; G.W.L.,

Y.S.J., and M.-S.C. performed the experiments; S.L., Y.I.K., S.S.L., and B.Y.C. analyzed the data; M.-S.C. and S.L. wrote the manuscript with the assistance and approval of all authors.

### Declaration of competing interest

The authors declare that they have no conflict of interest.

### Acknowledgements

This research was supported by the Nuclear R & D Program of the Ministry of Science, ICT and Future Planning (MSIP), Republic of Korea.

### Appendix A. Supplementary data

Supplementary data to this article can be found online at <https://doi.org/10.1016/j.plaphy.2019.10.008>.

### References

- Agati, G., Brunetti, C., Di Ferdinando, M., Ferrini, F., Pollastri, S., Tattini, M., 2013. Functional roles of flavonoids in photoprotection: new evidence, lessons from the past. *Plant Physiol. Biochem.* 72, 35–45.
- Bednar, R.A., Hadcock, J.R., 1988. Purification and characterization of chalcone isomerase from soybeans. *J. Biol. Chem.* 263, 9582–9588.
- Cheng, H., Li, L., Cheng, S., Cao, F., Wang, Y., Yuan, H., 2011. Molecular cloning and function assay of a chalcone isomerase gene (*GbCHI*) from *Ginkgo biloba*. *Plant Cell Rep.* 30, 49–62.
- Cheong, J.-J., Choi, Y.D., 2003. Methyl jasmonate as a vital substance in plants. *Trends Genet.* 19, 409–413.
- Clough, S.J., Bent, A.F., 1998. Floral dip: a simplified method for *Agrobacterium*-mediated transformation of *Arabidopsis thaliana*. *Plant J.* 16, 735–743.
- Conesa, A., Götz, S., García-Gómez, J.M., Terol, J., Talón, M., Robles, M., 2005. Blast2GO: a universal tool for annotation, visualization and analysis in functional genomics research. *Bioinformatics* 21, 3674–3676.
- Danaee, M., Farzinebrahimi, R., Kadir, M.A., Sinniah, U.R., Mohamad, R., Mat Taha, R., 2015. Effects of MeJA and SA elicitation on secondary metabolic activity, antioxidant content and callogenesis in *Phyllanthus pulcher*. *Braz. J. Bot.* 38, 265–272.
- Dixon, R.A., Richard Blyden, E., Robbins, M.P., Van Tunen, A.J., Mol, J.N., 1988. Comparative biochemistry of chalcone isomerases. *Phytochemistry* 27, 2801–2808.
- Dong, X., Braun, E.L., Grotewold, E., 2001. Functional conservation of plant secondary metabolic enzymes revealed by complementation of *Arabidopsis* flavonoid mutants with maize genes. *Plant Physiol.* 127, 46–57.
- Druka, A., Kudrna, D., Rostoks, N., Brueggeman, R., von Wettstein, D., Kleinhofs, A., 2003. Chalcone isomerase gene from rice (*Oryza sativa*) and barley (*Hordeum vulgare*): physical, genetic and mutation mapping. *Gene* 302, 171–178.
- Falcone Ferreyra, M.L., Rius, S., Casati, P., 2012. Flavonoids: biosynthesis, biological functions, and biotechnological applications. *Front. Plant Sci.* 3.
- Fouché, S.D., Dubery, I.A., 1994. Chalcone isomerase from *Citrus sinensis*: purification and characterization. *Phytochemistry* 37, 127–132.
- Gadzovska, S., Maury, S., Delaunay, A., Spasenowski, M., Joseph, C., Hagège, D., 2007. Jasmonic acid elicitation of *Hypericum perforatum* L. cell suspensions and effects on the production of phenylpropanoids and naphthodianthrones. *Plant Cell Tissue Org.* 89, 1–13.
- Ghasemzadeh, A., Talei, D., Jaafar, H.Z.E., Juraimi, A.S., Mohamed, M.T.M., Puteh, A., Halim, M.R.A., 2016. Plant-growth regulators alter phytochemical constituents and pharmaceutical quality in Sweet potato (*Ipomoea batatas* L.). *BMC Complement Altern. Med.* 16, 152–152.
- Grabherr, M.G., Haas, B.J., Yassour, M., Levin, J.Z., Thompson, D.A., Amit, I., Adiconis, X., Fan, L., Raychowdhury, R., Zeng, Q., Chen, Z., Mauceli, E., Hacohen, N., Gnirke, A., Rhind, N., di Palma, F., Birren, B.W., Nusbaum, C., Lindblad-Toh, K., Friedman, N., Regev, A., 2011. Full-length transcriptome assembly from RNA-Seq data without a reference genome. *Nat. Biotechnol.* 29, 644–652.
- Grotewold, E., Peterson, T., 1994. Isolation and characterization of a maize gene encoding chalcone flavanone isomerase. *Mol. Gen. Genet.* 242, 1–8.
- Guo, J., Zhou, W., Lu, Z., Li, H., Li, H., Gao, F., 2015. Isolation and functional analysis of chalcone isomerase gene from purple-fleshed sweet potato. *Plant Mol. Biol. Report.* 33, 1451–1463.
- Hong, L., Qian, Q., Tang, D., Wang, K., Li, M., Cheng, Z., 2012. A mutation in the rice chalcone isomerase gene causes the golden hull and internode 1 phenotype. *Planta* 236, 141–151.
- Hrazdina, G., Wagner, G.J., Siegelman, H.W., 1978. Subcellular localization of enzymes of anthocyanin biosynthesis in protoplasts. *Phytochemistry* 17, 53–56.
- Huang, Y., Niu, B., Gao, Y., Fu, L., Li, W., 2010. CD-HIT Suite: a web server for clustering and comparing biological sequences. *Bioinformatics* 26, 680–682.
- Jez, J.M., Bowman, M.E., Dixon, R.A., Noel, J.P., 2000. Structure and mechanism of the evolutionarily unique plant enzyme chalcone isomerase. *Nat. Struct. Biol.* 7, 786.
- Jiang, W., Yin, Q., Wu, R., Zheng, G., Liu, J., Dixon, R.A., Pang, Y., 2015. Role of a chalcone isomerase-like protein in flavonoid biosynthesis in *Arabidopsis thaliana*. *J. Exp. Bot.* 66, 7165–7179.
- Jung, J.H., Kim, H., Go, Y.S., Lee, S.B., Hur, C.-G., Kim, H.U., Suh, M.C., 2011. Identification of functional *BrFAD2-1* gene encoding microsomal delta-12 fatty acid desaturase from *Brassica rapa* and development of *Brassica napus* containing high oleic acid contents. *Plant Cell Rep.* 30, 1881–1892.
- Karimi, M., Inzé, D., Depicker, A., 2002. GATEWAY™ vectors for *Agrobacterium*-mediated plant transformation. *Trends Plant Sci.* 7, 193–195.
- Kim, H.B., Bae, J.H., Lim, J.D., Yu, C.Y., An, C.S., 2007. Expression of a functional type-I chalcone isomerase gene is localized to the infected cells of root nodules of *Elaeagnus umbellata*. *Mol. Cells* 23, 405–409.
- Kimura, Y., Aoki, T., Ayabe, S., 2001. Chalcone isomerase isozymes with different substrate specificities towards 6'-hydroxy- and 6'-deoxychalcones in cultured cells of *Glycyrrhiza echinata*, a leguminous plant producing 5-deoxyflavonoids. *Plant Cell Physiol.* 42, 1169–1173.
- Koornneef, M., 1990. Mutations affecting the testa colour in *Arabidopsis*. *Arabidopsis Inf. Serv.* 27, 1–4.
- Lee, E.M., Bai, H.-W., Lee, S.S., Hong, S.H., Cho, J.-Y., Lee, I.-C., Chung, B.Y., 2012. Stress-induced increase in the amounts of maysin and maysin derivatives in world premium natural compounds from centipede grass. *Radiat. Phys. Chem.* 81, 1055–1058.
- Li, F., Jin, Z., Qu, W., Zhao, D., Ma, F., 2006. Cloning of a cDNA encoding the *Saussurea medusa* chalcone isomerase and its expression in transgenic tobacco. *Plant Physiol. Biochem.* 44, 455–461.
- Li, J., Ma, J., Guo, H., Zong, J., Chen, J., Wang, Y., Li, D., Li, L., Wang, J., Liu, J., 2018a. Growth and physiological responses of two phenotypically distinct accessions of centipede grass (*Eremochloa ophiuroides* (Munro) Hack.) to salt stress. *Plant Physiol. Biochem.* 126, 1–10.
- Li, J., Zong, J., Chen, J., Wang, Y., Li, D., Li, L., Wang, J., Guo, H., Liu, J., 2018b. De novo assembly and comparative transcriptome analysis reveals genes potentially involved in tissue-color changes in centipede grass (*Eremochloa ophiuroides* [Munro] Hack.). *Plant Physiol. Biochem.* 130, 345–355.
- Long, M., Rosenberg, C., Gilbert, W., 1995. Intron phase correlations and the evolution of the intron/exon structure of genes. *Proc. Natl. Acad. Sci. U.S.A.* 92, 12495–12499.
- Mehdy, M.C., Lamb, C.J., 1987. Chalcone isomerase cDNA cloning and mRNA induction by fungal elicitor, wounding and infection. *EMBO J.* 6, 1527–1533.
- Mohamed, R.K., Gibril, A.Y., Rasmay, N.M.H., Abu-Salem, F.M., 2016. Extraction of anthocyanin pigments from *Hibiscus sabdariffa* L. and evaluation of their antioxidant activity. *Middle East J. Appl. Sci.* 6, 856–866.
- Mol, J.N.M., Robbins, M.P., Dixon, R.A., Veltkamp, E., 1985. Spontaneous and enzymic rearrangement of naringenin chalcone to flavanone. *Phytochemistry* 24, 2267–2269.
- Moore, J.P., Paul, N.D., Whittaker, J.B., Taylor, J.E., 2003. Exogenous jasmonic acid mimics herbivore-induced systemic increase in cell wall bound peroxidase activity and reduction in leaf expansion. *Funct. Ecol.* 17, 549–554.
- Morita, Y., Takagi, K., Fukuchi-Mizutani, M., Ishiguro, K., Tanaka, Y., Nitasaka, E., Nakayama, M., Saito, N., Kagami, T., Hoshino, A., Iida, S., 2014. A chalcone isomerase-like protein enhances flavonoid production and flower pigmentation. *Plant J.* 78, 294–304.
- Nakagawa, T., Suzuki, T., Murata, S., Nakamura, S., Hino, T., Maeo, K., Tabata, R., Kawai, T., Tanaka, K., Niwa, Y., Watanabe, Y., Nakamura, K., Kimura, T., Ishiguro, S., 2007. Improved gateway binary vectors: high-performance vectors for creation of fusion constructs in transgenic analysis of plants. *Biosci. Biotechnol. Biochem.* 71, 2095–2100.
- Ngaki, M.N., Louie, G.V., Philippe, R.N., Manning, G., Pojer, F., Bowman, M.E., Li, L., Larsen, E., Wurtele, E.S., Noel, J.P., 2012. Evolution of the chalcone-isomerase fold from fatty-acid binding to stereospecific catalysis. *Nature* 485, 530–533.
- Qin, J.C., Zhu, L., Gao, M.J., Wu, X., Pan, H.Y., Zhang, Y.S., Li, X., 2011. Cloning and functional characterization of a chalcone isomerase from *Trigonella foenum-graecum* L. *Planta Med.* 77, 765–770.
- Saslosky, D., Winkel-Shirley, B., 2001. Localization of flavonoid enzymes in *Arabidopsis* roots. *Plant J.* 27, 37–48.
- Shih, C.H., Chu, H., Tang, L.K., Sakamoto, W., Maekawa, M., Chu, I.K., Wang, M., Lo, C., 2008. Functional characterization of key structural genes in rice flavonoid biosynthesis. *Planta* 228, 1043–1054.
- Shimada, N., Aoki, T., Sato, S., Nakamura, Y., Tabata, S., Ayabe, S.-i., 2003. A cluster of genes encodes the two types of chalcone isomerase involved in the biosynthesis of general flavonoids and legume-specific 5-deoxy(iso)flavonoids in *Lotus japonicus*. *Plant Physiol.* 131, 941–951.
- Shin, J., Park, E., Choi, G., 2007. PIF3 regulates anthocyanin biosynthesis in an HY5-dependent manner with both factors directly binding anthocyanin biosynthetic gene promoters in *Arabidopsis*. *Plant J.* 49, 981–994.
- Shirley, B.W., Kubasek, W.L., Storz, G., Bruggemann, E., Koornneef, M., Ausubel, F.M., Goodman, H.M., 1995. Analysis of *Arabidopsis* mutants deficient in flavonoid biosynthesis. *Plant J.* 8, 659–671.
- Shoeva, O.Y., Khlestkina, E.K., Berges, H., Salina, E.A., 2014. The homologous genes encoding chalcone-flavanone isomerase in *Triticum aestivum* L.: structural characterization and expression in different parts of wheat plant. *Gene* 538, 334–341.
- Smith, J.V., Luo, Y., 2004. Studies on molecular mechanisms of *Ginkgo biloba* extract. *Appl. Microbiol. Biotechnol.* 64, 465–472.
- Soderlund, C., Descour, A., Kudrna, D., Bomhoff, M., Boyd, L., Currie, J., Angelova, A., Collura, K., Wissotski, M., Ashley, E., Morrow, D., Fernandes, J., Walbot, V., Yu, Y., 2009. Sequencing, mapping, and analysis of 27,455 maize full-length cDNAs. *PLoS Genet.* 5, e1000740.
- Tapas, A.R., Sakarkar, D.M., Kakde, R.B., 2008. Flavonoids as nutraceuticals: a review. *Trop. J. Pharm. Res.* 7, 1089–1099.
- Terai, Y., Fujii, I., Byun, S.-H., Nakajima, O., Hakamatsuka, T., Ebizuka, Y., Sankawa, U., 1996. Cloning of chalcone-flavanone isomerase cDNA from *Pueraria lobata* and its overexpression in *Escherichia coli*. *Protein Expr. Purif.* 8, 183–190.
- Trapp, S.C., Croteau, R.B., 2001. Genomic organization of plant terpene synthases and

- molecular evolutionary implications. *Genetics* 158, 811–832.
- Van Tunen, A.J., Mol, J.N., 1987. A novel purification procedure for chalcone flavanone isomerase from *Petunia hybrida* and the use of its antibodies to characterize the *Po* mutation. *Arch. Biochem. Biophys.* 257, 85–91.
- Wang, J., Qian, J., Yao, L., Lu, Y., 2015. Enhanced production of flavonoids by methyl jasmonate elicitation in cell suspension culture of *Hypericum perforatum*. *Bioresour. Bioprocess.* 2, 5.
- Winkel-Shirley, B., 2001. Flavonoid biosynthesis. A colorful model for genetics, biochemistry, cell biology, and biotechnology. *Plant Physiol.* 126, 485–493.
- Yang, Y., Li, R., Qi, M., 2000. In vivo analysis of plant promoters and transcription factors by agroinfiltration of tobacco leaves. *Plant J.* 22, 543–551.